PHYSICAL REVIEW B **82**, 220201(R) (2010)

Long-range magnetic order in the quasicrystalline approximant Cd_6Tb

R. Tamura,[1,*] Y. Muro,[2] T. Hiroto,[1] K. Nishimoto,[1] and T. Takabatake[2,3]
[1]*Department of Materials Science and Technology, Tokyo University of Science, Noda 278-8510, Japan*
[2]*Department of Quantum Matter, AdSM, Hiroshima University, Higashi-Hiroshima 739-8530, Japan*
[3]*Institute for Advanced Materials Research, Hiroshima University, Higashi-Hiroshima 739-8530, Japan*
(Received 26 September 2010; revised manuscript received 22 October 2010; published 8 December 2010)

We report the observation of a long-range magnetic order in a quasicrystalline approximant, i.e., Cd_6Tb, demonstrating that a spin glass is not the ground state for the binary approximant but localized spins on the vertices of an icosahedron become antiferromagnetically ordered below 24 K. The result is in contrast to the spin-glasslike behaviors reported for Cd-Mg-*R* quasicrystals composed of same icosahedral clusters.

DOI: 10.1103/PhysRevB.82.220201 PACS number(s): 75.50.Kj, 61.44.Br, 65.40.Ba

Quasicrystals[1] are distinguished from other forms of solids by their unique rotational symmetries such as fivefold, eightfold, tenfold, and 12-fold symmetries. One of the unsolved fundamental issues in the condensed-matter physics is to elucidate physical properties intrinsic to quasiperiodic arrangement of atoms, i.e., the quasiperiodicity.[2] In particular, magnetic properties of rare-earth (*R*) bearing quasicrystals such as Zn-Mg-*R* (*R*=Gd,Tb, Dy, Ho, and Er) (Refs. 3 and 4) and Cd-Mg-*R* (*R*=Gd, Tb, Dy, Ho, Er, Tm, and Yb) (Refs. 5 and 6) have received particular attention since they have well-localized magnetic moments located on a quasiperiodic sublattice providing quasiperiodic spin systems and have been expected to reveal unique magnetic orders due to the quasiperiodicity.[7] Contrary to such expectations, however, spin-glasslike freezing phenomena have been observed in the above magnetic quasicrystals but long-range magnetic order has never been reported up to date in either quasicrystals or their crystalline analogs, i.e., crystalline approximants. The present Rapid Communication reports the observation of a magnetic order in a crystalline counterpart, i.e., Cd_6Tb, composed of the same icosahedral cluster units as the Cd-Mg-*R* quasicrystals demonstrating that localized spins sitting on the vertices of an icosahedron become ordered at low temperatures. The result shows that a long-range magnetic order is possible in compounds made of rare-earth icosahedra and may suggest that it is also possible in the Cd-Mg-*R* quasicrystals having similar local environments composed of the same icosahedral clusters.

Cd_6Tb (Ref. 8) crystalline approximant, one of a huge family of isostructural Cd_6M (*M*=Ca, Sr, Y, Ce, Pr, Nd, Sm, Eu, Gd, Tb, Dy, Ho, Er, Tm, Yb, and Lu) compounds, is a bcc cubic crystal[9,10] composed of so-called Tsai-type icosahedral clusters,[11] which are regarded as the building blocks of stable binary quasicrystals, $Cd_{5.7}Yb$ (Ref. 12) and $Cd_{5.7}Ca$,[13] discovered in 2000 by Tsai *et al.* and their atomic structure has been determined in 2007 by Takakura *et al.*[14] A Tsai-type cluster is made of four successive shells: the first shell is a dodecahedron composed of 20 Cd atoms, the second shell an icosahedron of 12 Tb atoms, the third shell an icosidodecahedron of 30 Cd atoms, and the outermost shell a defect rhombic triacontahedron of 60 Cd atoms.[11] One of the biggest advantages to study binary systems such as Cd_6R (*R*=rare earth) is that they have no chemical disorders among the constituent elements since the *R* atoms occupy a single crystallographic site (24*g*) with full occupancy as illustrated in Fig. 1, i.e., they are exclusively situated at the vertices of the second icosahedron shell and the remaining seven sites are occupied by Cd atoms. This situation is in striking contrast to ternary systems such as Zn-Mg-*R* and Cd-Mg-*R*, where chemical disorders between rare earth (*R*) and other elements are essentially unavoidable as evidenced by their sizable single phase domains. Thus, the Cd_6R compounds can be regarded as ideal spin systems for investigations on the intrinsic magnetic property of compounds made of rare-earth icosahedra.

In the Cd_6R structures, the nearest neighbors are not *R*-*R* pairs but the *R* ions are separated from the nearest ones by ~0.6 nm, indicating that the magnetic interaction between the *R* ions is mediated by conduction electrons, i.e., Ruderman-Kittel-Kasuya-Yoshida interaction. There are two types of magnetic interactions in the Cd_6R compounds; one is an intracluster interaction and the other is an intercluster interaction. In Cd_6Tb, the nearest Tb-Tb distance (0.5713 nm) exists between neighboring clusters and the next-nearest Tb-Tb distance (0.5725 nm) exists inside the icosahedron shell. Thus, a long-range magnetic order may be regarded as a result of an interplay between these two competing interactions.

Recently, a series of large unit-cell compounds RFe_2Zn_{20} and RCo_2Zn_{20} (*R*=Y, Nd, Sm, and Gd-Lu) have been extensively investigated and diverse magnetic behaviors were re-

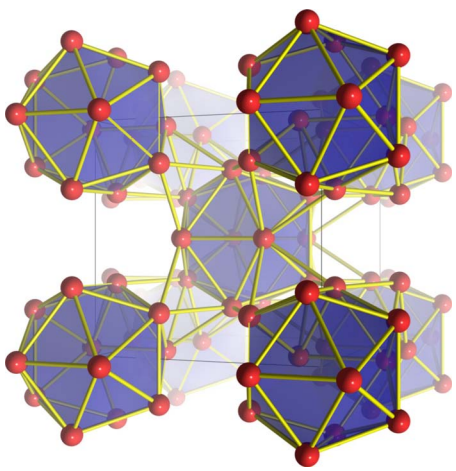

FIG. 1. (Color online) Tb sites in the unit cell of the Cd_6Tb cubic approximant. 12 Tb atoms occupy the second icosahedron shell of a Tsai-type cluster.

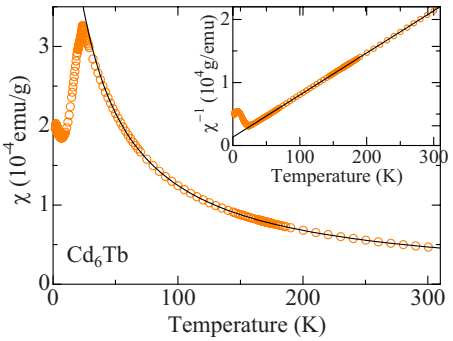

FIG. 2. (Color online) Magnetic susceptibility χ of Cd_6Tb from 1.8 to 300 K measured with the magnetic field of 1000 Oe. The solid line is a fit to the Curie-Weiss law between 50 and 300 K. The inset shows the inverse susceptibility of Cd_6Tb. The data are well fitted to the solid straight line showing that the Curie-Weiss law is obeyed above ~50 K.

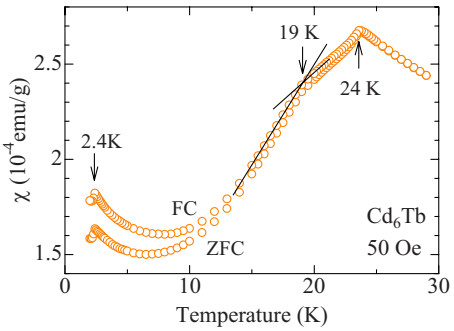

FIG. 3. (Color online) Magnetic susceptibility χ of Cd_6Tb in a low-temperature region from 1.8 to 30 K measured with the magnetic field of 50 Oe. The χ-T curve displays two anomalies at 24 and 2.4 K and one kink at 19 K as denoted by arrows showing an occurrence of successive magnetic transitions. FC and ZFC magnetic susceptibilities are shown.

ported depending on the rare-earth element.[15] Although they are not crystalline approximants, they have close structural similarities with the Cd_6R compounds in a sense that the R ions are fully surrounded by shells of nonmagnetic ions, i.e., Zn ions, with a similar R-R spacing of ~0.6 nm. It will be also of interest to make a comparison of magnetic properties between the two types of large unit-cell compounds from a structural point of view.

Alloys of a nominal composition, Cd_6Tb, are prepared by melting high-purity raw materials at 1000 K for 72 h in an alumina crucible sealed inside a quartz tube, followed by water quenching. The alloys were then annealed at 770 K for 100 h to improve the sample homogeneity as well as to reduce point defects to the thermal equilibrium level. We note that long-time annealing is indispensable for obtaining sharp magnetic transitions; magnetic transitions are easily smeared out in the presence of structural defects. The phase purity of the samples was examined by powder x-ray diffraction as well as by transmission electron microscopy. Magnetic properties were measured from 1.8 to 300 K by using a superconducting quantum interference device magnetometer [Quantum Design, MPMS (Magnetic Property Measurement System)] in magnetic fields up to 5 T and specific heat was measured in a relaxation method from 1.8 to 300 K. Electrical-resistivity measurements were performed by a four-probe method using ac resistance bridge from 1.9 to 300 K.

Figure 2 shows magnetic susceptibility of Cd_6Tb measured at 1000 Oe in a temperature range between 1. 8 and 300 K. In a high-temperature region above ~50 K, the susceptibility excellently obeys the Curie-Weiss law, i.e., $\chi = \frac{N_A \mu_{eff}^2}{3k_B(T-\Theta)}$, exhibiting a paramagnetic nature of Tb spins, as evidenced by a linear $1/\chi$-T relation shown in the inset. Here, N_A, μ_{eff}, k_B, and Θ are the Avogadro number, the effective moment, the Boltzmann constant, and the Weiss temperature, respectively. Results of a least-square fit to the Curie-Weiss law incorporating a temperature-independent term χ_0 are $\mu_{eff}=9.8\ \mu_B$, $\Theta=-17$ K, and $\chi_0=1.7 \times 10^{-6}$ emu/g. The obtained effective magnetic moment μ_{eff} is nearly equal to the theoretical value (9.72 μ_B) of the Tb^{3+} free ion. Thus, the Tb ions in Cd_6Tb are well localized in a trivalent state with weak crystalline electric field (CEF), which is qualitatively the same as the cases of Zn-Mg-Tb (Ref. 16) and Cd-Mg-Tb (Refs. 17 and 18) quasicrystals. The negative Θ value means that major interaction between spins is antiferromagnetic in the paramagnetic state. The obtained Θ value (−17 K) is close to the value (−24.5 to −23 K) reported for the Cd-Mg-Tb quasicrystal.[17,18]

Figure 3 shows magnetic susceptibility of Cd_6Tb in a low-temperature region below ~30 K. Occurrences of magnetic transitions are clearly evidenced by sharp anomalies in the χ-T curve: three anomalies are noticed at 24, 19, and 2.4 K, indicating an occurrence of three successive magnetic transitions. Here, the anomaly at 19 K is recognized as a kink in the χ-T curve. Figure 4 shows the field dependence of magnetization measured for the three magnetic phases as well as for the paramagnetic one above 24 K. With decreasing temperature, a metamagneticlike anomaly appears at 21 K as indicated by an arrow at 1.6 T, and the anomaly is observed to increase toward higher fields, i.e., 2.3 T, as temperature is lowered to 15 K. Here, the magnetic fields of the anomalies were determined from the position of the maximum slope of

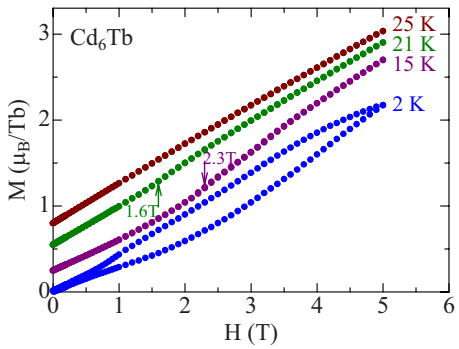

FIG. 4. (Color online) Magnetic field dependence of the magnetization M of Cd_6Tb measured for three magnetic phases as well as for the paramagnetic one. Arrows indicate metamagneticlike anomalies and their magnetic fields were determined from the position of the maximum slope of the M-T curve. The M-H curves at 15, 21, and 25 K are shifted vertically by 0.25 μ_B, 0.55 μ_B, and 0.8 μ_B, respectively, for clarity.

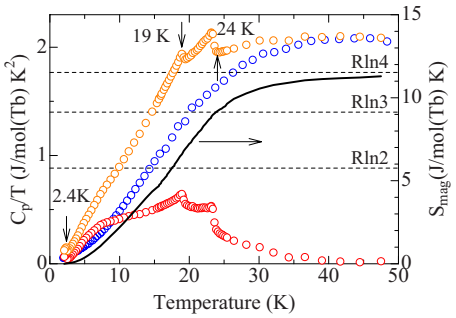

FIG. 5. (Color online) Temperature dependences of the specific heat C_p of Cd_6Tb (orange circles, top) and Cd_6Yb (blue circles, middle) plotted as C_p/T vs T. The magnetic contribution to specific heat C_m (red circles, bottom) is obtained by subtracting C_p/T of nonmagnetic Cd_6Yb from that of Cd_6Tb. The solid line represents magnetic entropy S_m obtained from integration of C_m/T. C_p of Cd_6Tb exhibits three anomalies at 24, 19, and 2.4 K as denoted by arrows, which corresponds to the anomalies observed in the χ-T curve.

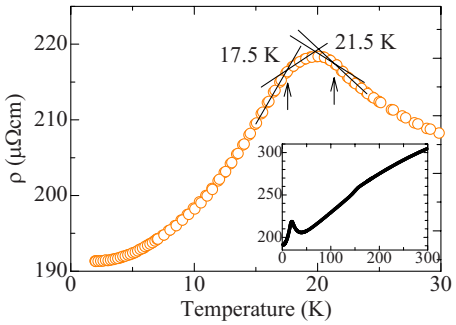

FIG. 6. (Color online) Electrical resistivity ρ of Cd_6Tb as a function of temperature in a range between 1.8 and 30 K for a different specimen. The inset shows the ρ-T curve of Cd_6Tb up to 300 K. The magnetic transitions at 24 and 19 K are recognized as changes in the slope of the ρ-T curve at 21.5 and 17.5 K as denoted by arrows. The slight differences in the anomaly temperatures from those observed in the magnetic and thermal measurements are possibly due to the sample dependence.

the M-H curve. Both the existence of the metamagneticlike anomaly and its shift toward higher fields with decreasing temperature clearly indicate that the transition at 24 K is antiferromagnetic one. On the other hand, the M-H curve at 2 K exhibits hysteresis between the magnetization and demagnetization curves. Such hysteresis is also noticed between field-cooled (FC) and zero FC (ZFC) susceptibilities as seen from Fig. 3. The origin of the hysteresis is not clear at the moment and hysteresis can occur from various mechanisms such as freezing of spins due to disorders, a frustrating nature of spins on an icosahedrons, etc. We note that the existence of disorders, probably vacancies, has been inferred from recent studies on isostructural Zn_6Sc.[19]

Figure 5 shows specific heat of Cd_6Tb in a low-temperature region below ~30 K. Occurrences of magnetic transitions are clearly observed by sharp anomalies in the specific heat: Three anomalies are noticed in the C/T-T curve at 24, 19, and 2.4 K, exactly at the same temperatures of the anomalies observed in the χ-T curve. Next, the magnetic contribution to C_p was estimated by subtracting C_p/T of nonmagnetic Cd_6Yb from that of Cd_6Tb. Their lattice contributions to C_p are expected to be nearly the same since Cd_6Yb is isostructural to Cd_6Tb. The magnetic entropy S_{mag} was estimated by the integration $\int_0^T \frac{C_{mag}}{T} dT$ and is plotted as a solid line in Fig. 5. The maximum magnetic entropy of Cd_6R is given by $S_{mag}=R\ln(2J+1)$ per mole (R^{3+}), where J is the total angular momentum of R^{3+}, i.e., $J=6$ for Tb^{3+}. The figure shows that S_{mag} reaches R ln 2 and R ln 3 at T_{N2} (19 K) and T_{N1} (24 K), respectively, converging to R ln 4 as T approaches 50 K. The gradual increase in S_{mag} toward R ln 4 above T_{N1} indicates the existence of a magnetic short-range order above T_{N1}. Since the Tb^{3+} ions occupy a single site with site symmetry m,[10] the $4f$ levels of a Tb^{3+} ion are split into 13 singlets due to the monoclinic CEF. The convergence of S_{mag} to R ln 4 indicates that the lowest $4f$ states are composed of nearly degenerate four singlets at ~50 K.

Figure 6 presents electrical resistivity of Cd_6Tb in a temperature range between 1.9 and 30 K measured for a different specimen and the inset shows the resistivity up to 300 K. As seen from the inset, a sharp cusp is observed at ~20 K, close to the onset of the antiferromagnetic order. The increase in the resistivity with decreasing temperature below ~40 K cannot be explained by a loss of scattering due to the magnetic ordering. For the origin of the anomaly, formation of a superzone gap may be responsible, which opens along the direction of the antiferromagnetic ordering due to a periodicity change.[20] On the other hand, the sharp decrease in the resistivity below 20 K is attributed to the loss of scattering due to the magnetic ordering. In Fig. 6, the successive transitions are recognized as slight changes in the slope in the ρ-T curve at 21.5 and 17.5 K. The transition at 2.4 K is not detected in the ρ-T curve, probably due to its small contribution to ρ.

As mentioned, Tb atoms occupy a single crystallographic site with full occupancy in binary Cd_6Tb as illustrated in Fig. 1, forming a 12-atoms icosahedron at the vertex and the body-center positions of the unit cell. Magnetic orders of the localized spins on the icosahedral site can be considered by placing a classical spin at each vertex of the icosahedron. In this view, the successive transitions indicate the existence of various antiferromagnetic spin configurations, which are nearly degenerate, over a bcc array of icosahedral clusters. Determination of the magnetic orders of Cd_6Tb is now an open issue and requires microscopic measurements such as neutron scattering. We note, however, that neutron experiments are difficult for Cd_6R since natural Cd is known to be a strong absorber of neutrons.

In conclusion, we have observed a long-range magnetic order in a crystalline approximant, i.e., Cd_6Tb. The result shows that a spin glass is not the ground state for the approximant but antiferromagnetic orders occur on a bcc array of icosahedral clusters. The present result also calls for detailed reexamination of a magnetic order in Cd-Mg-R quasicrystals since they have similar local environments composed of the same icosahedral clusters.

This work was supported by KAKENHI (under Grant No. 20045017) from the Ministry of Education, Culture, Sports, Science Technology of Japan.

*FAX: +81-4-7122-1499; tamura@rs.noda.tus.ac.jp

[1] D. Shechtman, I. Blech, D. Gratias, and J. W. Cahn, Phys. Rev. Lett. **53**, 1951 (1984).
[2] For a review, see *Physical Properties of Quasicrystals*, edited by Z. M. Stadnik (Springer-Verlag, Berlin, 1999).
[3] Z. Luo, S. Zhang, Y. Tang, and D. Zhau, Scr. Metall. Mater. **28**, 1513 (1993).
[4] A. P. Tsai, A. Niikura, A. Inoue, T. Masumoto, Y. Nishida, K. Tsuda, and M. Tanaka, Philos. Mag. Lett. **70**, 169 (1994).
[5] J. Q. Guo, E. Abe, and A. P. Tsai, Philos. Mag. Lett. **81**, 17 (2001).
[6] J. Q. Guo, E. Abe, and A. P. Tsai, Jpn. J. Appl. Phys., Part 2 **39**, L770 (2000).
[7] For a review, see T. J. Sato, Acta Crystallogr., Sect. A: Found. Crystallogr. **61**, 39 (2005).
[8] I. Johnson, R. Schablaske, B. Tani, and K. Anderson, Trans. Metall. Soc. AIME **230**, 1485 (1964).
[9] G. Bruzzone, M. L. Fornasini, and F. Merlo, J. Less-Common Met. **30**, 361 (1973).
[10] S. Y. Piao, C. P. Gómez, and S. Lidin, Z. Naturforsch., B: Chem. Sci. **61b**, 644 (2006).
[11] C. P. Gómez and S. Lidin, Phys. Rev. B **68**, 024203 (2003).
[12] A. P. Tsai, J. Q. Guo, E. Abe, H. Takakura, and T. J. Sato, Nature (London) **408**, 537 (2000).
[13] J. Q. Guo, E. Abe, and A. P. Tsai, Phys. Rev. B **62**, R14605 (2000).
[14] H. Takakura, C. P. Gómez, A. Yamamoto, M. D. Boissieu, and A. P. Tsai, Nature Mater. **6**, 58 (2007).
[15] S. Jia, N. Ni, S. L. Bud'ko, and P. C. Canfield, Phys. Rev. B **80**, 104403 (2009).
[16] I. R. Fisher, K. O. Cheon, A. F. Panchula, P. C. Canfield, M. Chernikov, H. R. Ott, and K. Dennis, Phys. Rev. B **59**, 308 (1999).
[17] T. J. Sato, J. Q. Guo, and A. P. Tsai, J. Phys.: Condens. Matter **13**, L105 (2001).
[18] S. E. Sebastian, T. Huie, I. R. Fisher, K. W. Dennis, and M. J. Kramer, Philos. Mag. **84**, 1029 (2004).
[19] T. Yamada, R. Tamura, Y. Muro, K. Motoya, M. Isobe, and Y. Ueda, Phys. Rev. B **82**, 134121 (2010).
[20] C. Sekine, T. Uchiumi, I. Shirotani, K. Matsuhira, T. Sakakibara, T. Goto, and T. Yagi, Phys. Rev. B **62**, 11581 (2000).